

# 裂解炉管焊接残余应力场中裂纹扩展行为的数值分析

祝金丹<sup>1</sup>, 张礼敬<sup>2</sup>, 巩建鸣<sup>2</sup>

(1. 南京化工职业技术学院 机械系, 南京 210048;

2. 南京工业大学 机械与动力工程学院, 南京 210009)

**摘 要:** 针对裂解炉管对接焊接热影响区中常见的环向与斜裂纹在焊接残余应力的作用下的扩展行为进行数值预测。采用基于 VNA 算法的有限单元交互法 (FEAM), 结合有限元方法研究焊接残余拉应力对炉管裂纹扩展的影响, 通过研究裂纹尖端区域的应力强度因子的变化来判断裂纹的准静态扩展倾向。结果表明, 在多道焊接焊接残余应力的影响下, 在炉管焊缝热影响区内表面的环向裂纹有沿环向变长的倾向, 而斜裂纹则同时有变长、变深的倾向。

**关键词:** 裂解炉管; 残余应力; 有限单元交互法; 有限元方法; 裂纹扩展

**中图分类号:** TG404 **文献标识码:** A **文章编号:** 0253-360X(2008)05-0101-05



祝金丹

## 0 序 言

在 HP40Nb 裂解炉管对接焊接过程中, 高梯度的温度分布以及材料的非线性响应促成的焊接残余应力是不可避免的。拉伸残余应力的存在会增加焊接结构开裂驱动力、降低结构的抗脆性断裂性能, 从而对焊接结构的完整性产生不利影响<sup>[1]</sup>。残余拉应力与炉管恶劣的服役条件交互作用增加了应力腐蚀开裂 SCC (stress corrosion cracking) 或疲劳开裂倾向。同时 SCC 裂纹的触发会导致炉管高温蠕变开裂<sup>[2]</sup>。采用基于 VNA 算法的数值求解技术 (有限单元交互法, finite element alternating method, FEAM) 研究焊接拉伸残余应力对炉管连接件焊缝区域裂纹扩展的影响, 通过研究裂纹尖端区域的应力强度因子的变化来判断裂纹的准静态扩展倾向。

## 1 裂解炉管中的裂纹

图 1 为裂解炉管对接焊缝区域常见的表面裂纹宏观形态, 主要存在两种裂纹状态即与焊缝方向成一夹角的斜表面裂纹和平行于焊缝的环向表面裂纹。测得的不同服役管龄的裂解炉管其裂纹损伤层厚度 (裂纹深度) 最深处可达 0.44 mm (内壁)。由于焊接残余应力的存在, 轴向残余拉应力是影响平行

于焊缝的环向裂纹开裂的主要驱动力, 而斜裂纹的开裂则是轴向与环向残余拉应力共同作用的。

## 2 有限单元交互法

### 2.1 FEAM 技术

使用有限元方法研究裂纹扩展问题无法保证对裂尖扩展方向的捕捉, 且通常需要花费大量的时间用于裂纹的网格划分 (尤其是裂尖区域的网格), 因而有限元方法处理裂纹问题目前仍有较大困难。由 Atluri 等人<sup>[3,4]</sup> 提出的有限单元交互法则对复杂结构含裂纹受载问题求解具有明显的优势。其基本思想是: 先通过有限元方法求解出无裂纹结构在受载时裂纹所在位置处的载荷分布, 然后使用解析法求解出裂纹无限体为平衡上述裂纹处载荷所需外力, 得到的外力作用于无裂纹结构上再次进行有限元分析, 如此重复直至实现在无裂纹结构裂纹对应位置的载荷为零, 即裂纹自由表面状态 (图 2)。对无限区域内含裂纹问题的求解是基于 VNA 方法<sup>[5]</sup>。FEAM 技术已被成功用于解决多种结构表面裂纹及互约束多裂纹问题。

### 2.2 VNA 算法

假设  $x_1$  和  $x_2$  为椭圆裂纹所在平面内正交的两个方向,  $x_3$  为平面法线,  $a_1$ ,  $a_2$  与  $a_3$  为椭圆三个半轴长, 对于平面椭圆裂纹 (图 3),  $a_3 = 0$ , 令裂纹表面力沿着椭圆面表示为

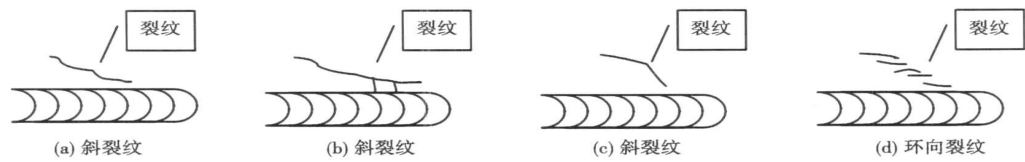


图 1 损伤炉管焊接裂纹宏观形态  
Fig. 1 Schematic of cracks near weld of pyrolysis tube

最高阶相关。  
对受任意裂纹表面力的无限体椭圆裂纹, 其裂纹表面法线方向的势函数由 Trefftz 公式<sup>[3]</sup> 表述为

$$f_3 = \sum_{i=0}^1 \sum_{j=0}^1 \sum_{k=0}^M \sum_{l=0}^k C_{3, k-l}^{(i, j)} l F_{2k-2l+i, 2l+j} \quad (2)$$

式中:  $C$  为待定矩阵;  $F$  为基本势函数, 其详细解见文献[6];  $k, l$  为受  $M$  控制的任意整数。应力分量  $R_{ij}$  和位移分量可以用势函数方程表示。将应力以矩阵形式表示为

$$\{R\}_{6 \times 1} = [P]_{6 \times N} \{C\}_{N \times 1} \quad (3)$$

式中:  $[P]$  为坐标  $(x_1, x_2, x_3)$  的函数;  $N$  为系数  $A$  与  $C$  的总数。为满足裂纹表面的边界条件, 参数  $A$  与  $C$  必须满足

$$\{A\}_{N \times 1} = [B]_{N \times N} \{C\}_{N \times 1} \quad (4)$$

式中:  $[B]$  的详细表达式见文献[3]。

由式(1)得到系数矩阵  $A$ , 然后由式(4)即可求得  $C$ 。 $C$  被确定, 第一类裂纹的应力强度因子  $K_I$  可以通过以下公式计算

$$K_I = 8\mu \left(\frac{\pi}{a_1 a_2}\right)^{1/2} \frac{Q^{1/4}}{a_1 a_2} H \quad (5)$$

$$Q = a_1^2 \sin^2 \theta + a_2^2 \cos^2 \theta \quad (6)$$

$$H = \sum_{i=0}^1 \sum_{j=0}^1 \sum_{k=0}^M \sum_{l=0}^k (-2)^{2k+i+j} (2k+i+j+1)! \left(\frac{\cos \theta}{a_1}\right)^{2k-2l+i} \left(\frac{\sin \theta}{a_2}\right)^{2l+j} C_{3, k-l}^{i, j} \quad (7)$$

式中:  $\theta$  为图 3 中表示的椭圆角;  $\mu$  为剪切模量。

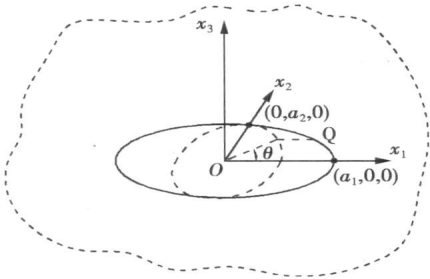


图 3 无限体中的椭圆裂纹  
Fig. 3 Elliptical crack in infinite body

2.3 FEAM 流程

使用 ABAQUS 进行裂解炉管焊接残余应力分析, 使用 Fortran 编写的 FEAM 子程序包含 VNA 程序调用有限元解并求解裂纹应力强度因子 (stress intensity factors, SIFs)。有限元无裂纹模型中的积分点处的残余应力连同裂纹尺寸 ( $a_1, a_2$  与  $\theta$ ) 被做为初始条件数据导入 FEAM 子程序, 将有限元模型中待研究裂纹区域积分点的残余应力分布通过多项式化处理, 通过 VNA 程序计算此次迭代中的应力强度因子同时解析得到无限体模型的载荷。将此载荷取反值作为下一次无裂纹有限元模型的外载荷重新进行有限元计算, 如此迭代, 直到满足解析无限体裂纹的

自由表面条件为止,裂纹端线的应力强度因子取各次迭代过程应力强度因子的总和。

3 裂解炉管焊接残余应力及表面裂纹

3.1 炉管残余应力与表面裂纹

高温服役的裂解炉管在线焊接方式为夹具夹持两炉管,然后对接焊接完成,两对接炉管尺寸相同( $\phi 164\text{ mm}\times 6.5\text{ mm}$ ),焊接坡口形式为 V 形,裂解炉管材料为 HP40Nb,属耐热不锈钢。由 ABAQUS 有限元软件完成热-力模拟分析,得到炉管焊接残余应力分布,其多道焊模拟思路及方法有效性见文献[7]。从其焊后残余应力分布规律来看,热影响区轴向与环向残余应力在内表面为拉应力,外表面为压应力。经现场检测到的炉管表面裂纹主要分布在接头热影响区(图 1),有斜表面裂纹和环向表面裂纹两类。由此可知,存在残余拉应力分布的炉管接头热影响区最易诱发裂纹扩展。而此区域将作为残余应力场中含裂纹问题的研究重点。

两种表面裂纹定义如图 4 所示,图中仅画出半裂纹。假设裂纹为椭圆裂纹,以两轴长来表征裂纹尺寸。环向裂纹平行于焊缝中心平面,而斜裂纹则与焊缝中心平面成  $\beta$  角( $\beta=45^\circ$ )。 $a_1, a_2$  为椭圆裂纹的长半轴与短半轴,也就是裂纹的半长与深度。 $a_2/a_1$  的值在 0.2~0.8 之间。裂纹中心点位于距焊

缝中心线 4.5 mm 处。通过 FEAM 计算裂纹端线(环向裂纹:  $\theta=0^\circ\sim 90^\circ$ ; 斜裂纹:  $\theta=0^\circ\sim 180^\circ$ )的应力强度因子分布,并通过改变  $a_1$  与  $a_2$  来研究相同残余应力场中裂纹尺寸变化对应力强度因子的影响,进而判断裂纹的扩展行为。

3.2 斜裂纹问题的处理

Mu 等人[8]在使用 FEAM 分析时将裂纹表面载荷分为垂直载荷与剪切载荷,根据各自载荷所使用的势函数的不同,可分别求解出各自方向的裂纹应力场与应力强度因子。同时认为这两种载荷作用互不干扰,可分别得到三类应力强度因子  $K_I, K_{II}$  和  $K_{III}$ 。因此,当对复杂载荷进行裂纹分析时,由 ASME 锅炉与压力容器标准规定[9],筒体内的斜裂纹可以通过正交投影到筒体的径向与轴向平面上。可得到投影于炉管模型的直角坐标系平面的环向与轴向裂纹,如图 5 所示。图中  $a_1$  与  $a_2$  分别为椭圆裂纹的长半轴与短半轴,下角标 O, L, T 分别表示原裂纹、投影后的环向裂纹与轴向裂纹,  $R_i$  为管内径(75.5 mm),  $t$  为管壁厚度 6.5 mm。

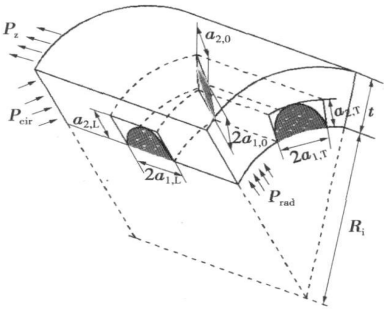


图 5 斜裂纹及其正交投影  
Fig. 5 Orthogonal projection for inclined crack

4 残余应力场中表面裂纹扩展行为

4.1 环向裂纹应力强度因子及扩展行为

使用 FEAM 方法计算得到的残余应力场中裂解炉管内表面热影响区不同深度和不同尺寸表面裂纹( $a_2/a_1=0.5$ )的沿裂纹端线的应力强度因子变化见图 6,图 7 所示。由图 6 可知,在相同裂纹长度下,环向裂纹越深,应力强度因子在裂纹最深处( $\theta\approx 90^\circ$ )下降越快,甚至达到负值,在半裂纹范围内,其应力强度因子的变化也越大;在裂纹端线表面附近( $\theta\approx 15^\circ$ ),随裂纹深度的增加,应力强度因子也迅速增加,在炉管接头热影响区残余拉应力作用下,此位置最容易诱发裂纹扩展。这说明在炉管内表面焊接残余拉应力的作用下,一个小的环向表面裂纹很有可

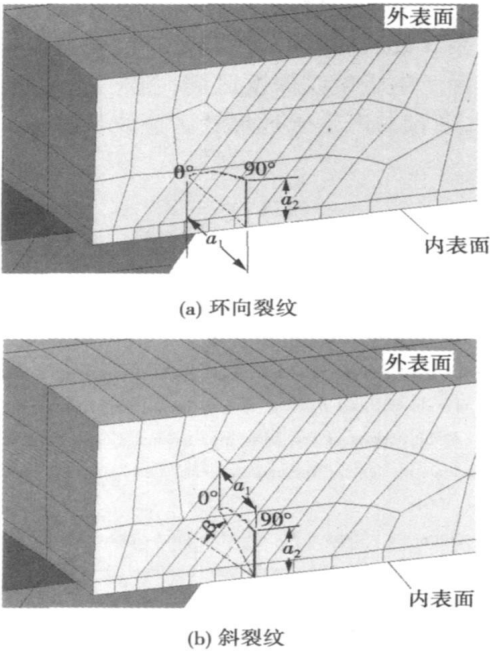


图 4 炉管内表面宏观裂纹示例  
Fig. 4 An example for surface crack of pyrolysis tube

能发展成为浅而长的表面裂纹。另一方面,当裂纹深度达到炉管壁厚的一半时,残余轴向与环向应力已变小甚至过渡到压应力时,由于压缩残余应力起主导作用,向深度方向的扩展受到抑制,同样说明此环向裂纹容易向长裂纹扩展。图 7 同样说明,尺寸较大的内表面环向裂纹倾向于发展为长裂纹,而对于小裂纹,沿裂纹端线应力强度因子值较小且变化不大,这种情况下裂纹扩展倾向不明了。

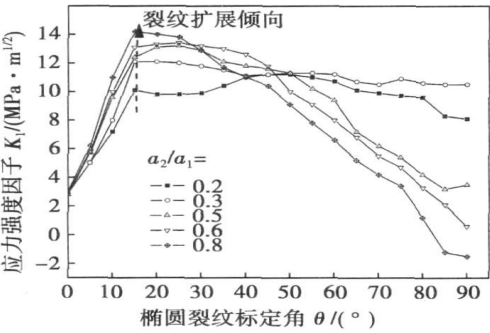


图 6 不同深度裂纹的应力强度因子( $a_1=1.0\text{ mm}$ )  
Fig. 6 SIFs for cracks with different depth( $a_1=1.0\text{ mm}$ )

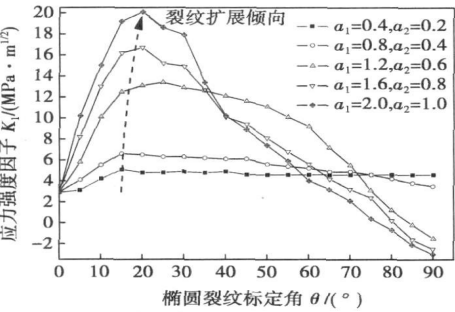


图 7 不同长度裂纹的应力强度因子( $a_2/a_1=0.5$ )  
Fig. 7 SIFs for cracks with different length( $a_2/a_1=0.5$ )

4.2 斜裂纹应力强度因子及扩展行为

对于斜裂纹,三个主方向的残余应力对裂纹的扩展作用都不容忽视。因而,在复杂应力作用下,斜裂纹不仅容易发生“张开型开裂”(K<sub>I</sub>),同样可能发生“滑开型开裂”(K<sub>II</sub>)或“撕开型开裂”(K<sub>III</sub>)。图 8 显示了三种裂纹深度应力强度因子的变化。由于斜裂纹中两部分半裂纹( $\theta=0^\circ\sim90^\circ$ 与 $\theta=90^\circ\sim180^\circ$ )所处的应力场在轴向与径向残余应力上有区别,前后半椭圆裂纹的应力强度因子会不尽相同。图 8 可以看出,在 $\theta\approx160^\circ$ 区域,第一类应力强度因子 K<sub>I</sub> 相对较大,容易从此点位置发生张开型裂纹扩展,且倾向于扩展成为长裂纹;第二类应力强度因子 K<sub>II</sub> 在裂纹深度区域( $\theta=40^\circ\sim120^\circ$ )值相对较大,但在此区

域变化不大,说明这个较宽的区域都容易诱发滑开型裂纹扩展,倾向于深度方向扩展;在 $\theta\approx0^\circ$ 点,即在炉管内表面上椭圆裂纹长轴端应力强度因子最大,倾向于长裂纹扩展。同样,较深的裂纹有着更大的裂纹扩展倾向。

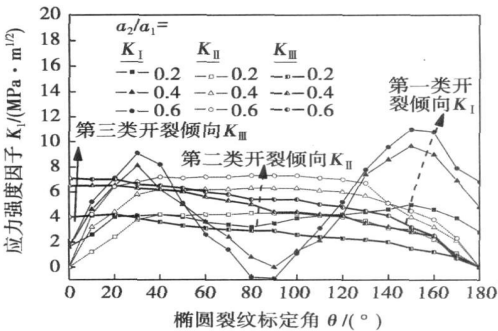


图 8 不同深度斜裂纹的应力强度因子( $a_1=1.5$ )  
Fig. 8 SIFs for inclined cracks with different depth( $a_1=1.5$ )

5 结 论

- (1) 内表面环向裂纹在残余拉应力的作用下倾向于扩展成为长裂纹,裂纹的深度增加,环向裂纹扩展倾向性增加。尺寸较大的内表面环向裂纹倾向于发展为长裂纹,而对于小裂纹,沿裂纹端线应力强度因子值较小且变化不大,裂纹扩展倾向不明了。
- (2) 内表面斜裂纹,第一类开裂容易发生在近焊缝区裂纹近表面区域,倾向于扩展长裂纹;第二类开裂容易产生于裂纹深度区域;第三类开裂倾向于长裂纹,最容易产生于远焊缝区裂纹长轴端(炉管内表面)。

参考文献:

[ 1 ] 涂善东. 高温结构完整性原理[ M ]. 北京: 科学出版社, 2003.  
[ 2 ] Bust F W, Zhang J, Dong P. Pipe and pressure vessel cracking: the role of weld induced residual stresses and creep damage during repair [ C ] //Transactions of the 14th International Conference on Structural Mechanics in Reactor Technology (SMiRT 14), Lyon, France 1997: 297-306.  
[ 3 ] Vijayakumar K, Atluri S N. An embedded elliptical crack in an infinite solid subject to arbitrary crack face tractions[ J ]. Journal of Applied Mechanics. 1981, 103(1): 88-96.  
[ 4 ] Nishioka T, Atluri S N. Analytical solution for embedded elliptical cracks and finite element alternating method for elliptical surface cracks subjected to arbitrary loadings[ J ]. Engineering Fracture Mechanics. 1983, 17(3): 247-268.

的影响[J]. 中国有色金属学报, 2003, 13(4): 1001—1004.

[2] 夏志东, 雷永平, 史耀武. 绿色高性能无铅钎料的研究与发展[J]. 电子工艺技术, 2002, 23(5): 185—191.

[3] 庄鸿寿. 无铅软钎料的新进展[J]. 电子工艺技术, 2001, 22(5): 192—196.

[4] 张文典. 实用表面组装技术[M]. 北京: 电子工业出版社, 2006.

[5] Yoshiharu K, Naomi W, William P. Tin pest in Sn—0.5Cu lead—free solder [J]. Journal of Material, 2001(6): 39—41.

[6] 赵小艳, 赵麦群, 王秀春, 等. Cu 和 Ce 对 Sn—Zn 系钎料合金物理性能和化学性能的影响[J]. 新技术新工艺, 2007(1): 62—64.

[7] 马 鑫, 何 鹏. 电子组装中的无铅软钎焊技术[M]. 哈尔

滨: 哈尔滨工业大学出版社, 2006.

[ 8] 菅沼克昭. 无铅焊接技术[M]. 宁晓山, 译. 北京: 科学出版社, 2004.

[9] 李树丰, 赵高阳. 等温时效对 Sn3.0Ag2.8Cu/Cu 焊点界面层组织的影响[J]. 机械工程材料, 2005 29(11): 21—24.

[ 10] Won K C, Huuck M L. Effect of soldering and aging time on interfacial microstructure and growth of intermetallic compounds between Sn—3.5Ag solder alloy and Cu substrate[ J]. Journal of Electronic Materials, 2000, 29(10): 1207—1213.

---

**作者简介:** 陈雷达, 男, 1982 年出生, 硕士研究生。主要研究方向为电子封装无铅钎料。发表论文 1 篇。

**Email:** chenld1982@sina.com

[ 上接第 104 页]

[5] Nishioka T, Kato T. An alternating method based on the VNA solution for analysis of damaged solid containing arbitrary distributed elliptical microcracks[J]. International Journal of Fracture, 1999, 97(1—4): 137—170.

[6] Kamaya M, Nishioka T. Evaluation of stress intensity factors by finite element alternating method[ C] // PVP: RPV Integrity and Fracture Mechanics. ASME/JSME, San Diego, US, 2004: 113—120.

[7] 陈 虎, 巩建鸣, 涂善东. 典型封闭环焊缝多道焊焊接残余应力的模拟分析[J]. 焊接学报, 2006, 27(10): 73—76.

[ 8] Mu Ruijia, Reddy D V. Stress intensity factors and weight functions for semi—elliptical cracks using finite element alternating method[ J]. Engineering Fracture Mechanics, 1994, 48(3): 305—323.

[9] ASME. New York, USA, FC—2400—3—2001. ASME boiler and pressure vessel code section XI[ S].

---

**作者简介:** 祝金丹, 女, 1980 年出生, 硕士研究生。主要从事机械制造(模具)及机械设计 CAD/CAE/CFD 方面的研究。发表论文 3 篇。

**Email:** zjd819@163.com

Guilian<sup>2</sup> (1. School of Materials Science and Engineering, Dalian University of Technology, Dalian 116024, Liaoning, China; 2. Research and Development Center, Wuhan Iron & Steel (Group) Corporation, Wuhan 430080, China). p93–96, 100

**Abstract:** The experiments were carried out upon the determination of SH–CCT diagrams and the characteristics of microstructures and properties in simulated coarse grain heat-affected zone (CGHAZ) of hot continuously rolled copper-bearing steel under single and double welding thermal cycles using thermal simulation. The results show that with the help of SH–CCT diagram of copper-bearing steel, it is proposed to choose  $t_{8/5}$  ranging from 7 s to 35 s during welding. The copper-bearing steel has a narrow range of heat-input and brittleness is easy to happen in the region of CGHAZ with higher heat-input. Granular bainite transformed from austenite leads to brittleness. Softening starts when  $t_{8/5}$  is more than 7 s. The dissolution of  $\epsilon$ –Cu, coarse lath bainite and more ferrite cause softening. Moreover, the impact toughness decreases dramatically and obvious brittleness happens in the intercritical region of CGHAZ. The reason is pearlite formed on the interface of original austenite and coarse granular bainite, which can reduce the impact toughness.

**Key words:** copper-bearing age-hardening steel; coarse grain heat-affected zone; SH–CCT; softening; brittleness

**Submerged-arc welding agglomerated flux for pressure vessel of anti-H<sub>2</sub>S corrosion** ZONG Lin<sup>1</sup>, WANG Zongjie<sup>2</sup> (1. School of Mechanical Engineering, Shenyang Institute of Chemical Technology, Shenyang 110142, China; 2. School of Materials and Science Engineering, Shenyang University of Technology, Shenyang 110023, China). p97–100

**Abstract:** Through analyzing slag system, alkalinity and chemical compositions of the deposited metal, a submerged-arc welding agglomerated flux for pressure vessel of anti-H<sub>2</sub>S corrosion with Al<sub>2</sub>O<sub>3</sub>–CaF<sub>2</sub>–MgO–SiO<sub>2</sub>–MnO–TiO<sub>2</sub> fluoride and alkaline type slag system was developed. The experimental results indicate that agglomerated flux matched two kinds of welding wire made in institute of metal research Chinese academy of sciences can both produce high tensile strength and low temperature impact toughness and good properties of the resistance to H<sub>2</sub>S corrosion. For matching the 1<sup>#</sup> welding wire, the weld metal have a relatively large component of Mn, brings down the  $\gamma \rightarrow \alpha$  transformation temperature, acicular ferrite increases in the weld metal. Thereby, the welded metal have higher low-temperature impact toughness. The low content of C, S and P has contributions to enhance the strength and impact toughness of the weld metal. The content of oxygen is only 0.035% and nitrogen is only 0.008%. The oxygen content reduces, which causes to produce bigger dimples in the ductile fracture appearance. At the same time the number of acicular ferrite increases, so the impact toughness is enhanced.

**Key words:** agglomerated flux; anti-corrosion; strength and toughness; chemical composition

**Numerical simulation on cracking growth behavior under effect of residual stresses in welding of pyrolysis tube** ZHU Jindan<sup>1</sup>, ZHANG Lijing<sup>2</sup>, GONG Jianming<sup>2</sup> (1. Mechanical Technology Department, Nanjing College of Chemical Technology, Nanjing

210048, China; 2. School of Mechanical and Power engineering, Nanjing University of Technology, Nanjing 210009, China). p101–104, 108

**Abstract:** This present focuses on the numerical prediction about the cracking growth behavior of circumferential and inclined cracks generally observed in the region of heat-affected zone on the effect of residual stresses of butt-welding of pyrolysis tube. Finite element alternating method (FEAM) based on VNA algorithm combining with finite element modeling was utilized to investigate the effect of residual stress on cracking and predict the cracking growth tendency according to the variation of stress intensity factors along the crack edge. The results show that under the effect of welding residual stresses, the circumferential cracks may tend to circumferentially lengthen along the major axis of crack, and both lengthening along major axis and being deep along minor axis of inclined crack may occur.

**Key word:** pyrolysis tube; residual stress; FEAM; FEM; cracking growth

**Influence of Sb on Sn–0.7Cu solder's melting point and soldering interface** CHEN Leida, MENG Gongge, LIU Xiaojing, LI Zhengping (School of Materials Science & Engineering, Harbin University of Science and Technology, Harbin 150040, China). p105–108

**Abstract:** The influences of Sb (0.25%, 0.5%, 0.75% and 1.0%) on Sn–0.7Cu lead-free solder's melting point and soldering interface was studied by scanning electron microscope and differential scanning calorimetry equipment. The result indicates that the melting point raises from 226.38 °C to 227.09 °C as Sb was added into the SnCu solders from 0.25% to 1.0%. But the melting point changed a little when Sb is less than 0.75%, only when its content comes up to 1.0% the melting point changed obviously. When SnCu solder contains 0.5% Sb, the pattern of IMC (intermetallic compound) changes obviously, scalloped IMC becomes smooth and the thickness of IMC becomes small and big prismatical Cu<sub>6</sub>Sn<sub>5</sub> is avoided; the growth of IMC is inhibited and the grain is refined. When more than 0.5% Sb is added into the solder, the big prismatical Cu<sub>6</sub>Sn<sub>5</sub> is formed again and IMC becomes thicker. The spiece of IMC wasn't changed when Sb is added into Sn–0.7Cu solder.

**Key words:** lead-free solder; melting point; soldering interface

**Effects of time interval in rapid prototyping of Al-alloy based on welding** SHEN Junqi, HU Shengsun, LIU Wanglan, HAN Jinghua (School of Materials Science and Engineering, Tianjin University, Tianjin 300072, China). p109–112

**Abstract:** In the process of rapid prototyping based on welding, heat input has great effect on the quality and capability of workpieces. Time interval of deposited layers is used as a method of controlling the heat input in rapid prototyping process of 5356 Al-alloy based on AC gas tungsten arc welding (AC-GTAW). Under the condition of various time interval of deposited layers, the surface morphologies and microstructures of deposited layers are better than that in equal time interval of deposited layers.

**Key words:** rapid prototyping based welding; AC gas tungsten arc welding; Al-alloy; time interval of deposited layers